Spectroscopic Characterization of Triple-Decker Lanthanide Porphyrin Sandwich Complexes. Effects of Strong $\pi\pi$ Interactions in Extended Assemblies

John K. Duchowski and David F. Bocian*

Contribution from the Department of Chemistry, Carnegie-Mellon University, Pittsburgh, Pennsylvania 15213. *Received April 20, 1990*

Abstract: Electrochemical, optical absorption, near-infrared, infrared, resonance Raman, and electron paramagnetic resonance data are reported for several neutral and singly oxidized triple-decker lanthanide porphyrin sandwich complexes $Ln_2(OEP)_3$ (Ln = La(III), Ce(III), Eu(III); OEP = octaethylporphyrin). The data indicate that there are strong $\pi\pi$ interactions between the porphyrin macrocycles in all of the complexes. As a consequence, the hole in the porphyrin π system of the $Ln_2(OEP)_3^+$ systems is delocalized over all three rings on the vibrational and electronic time scales. The singly oxidized complexes exhibit a characteristic electronic absorption band at very low energies (ca. 2200 nm). This absorption arises as a direct consequence of the strong $\pi\pi$ interactions between the rings. A molecular orbital scheme is proposed that accounts for this low-energy feature as well as a number of other properties of the triple-decker sandwich complexes.

I. Introduction

Stacked and bridged porphyrinic assemblies exhibit unusual optical, redox, electron-transfer, and conductivity properties due to strong $\pi\pi$ interactions between the macrocycles.[1-17] We and others have been investigating the consequences of these interactions in a variety of neutral and single-hole (both neutral radicals and cation radicals) complexes of the form $Ln(P)_2$ (Ln = lanthanide; P = porphyrin).[14c,f-h,15a,b,17] Several studies of the analogous actinide complexes have also been reported.[15c,16] In the case of certain neutral actinide sandwich complexes, the close proximity of the porphyrin rings results in novel, low-energy fluorescence features.[15c] In the case of all the single-hole complexes, the strong $\pi\pi$ interactions between the macrocycles result in complete delocalization of the hole over the porphyrin π system on the vibrational and electronic time scales. We have recently proposed a molecular orbital model for the double-decker lanthanide porphyrins that accounts for this delocalization and provides insight into the redox and spectroscopic properties of these complexes in general.[17]

In the course of their investigations on $Ln(P)_2$ complexes, Buchler and co-workers demonstrated that these π assemblies can be extended to triple deckers of the form $Ln_2(P)_3$.[14b,d,e,i] Crystallographic studies on $Ce_2(OEP)_3$ indicate that the macrocycles are rotated with respect to one another such that the two structurally equivalent outer rings are in registry (eclipsed), while the inner ring is rotated by ~45° with respect to the outer rings (staggered).[14d] The Ce(III) ions are closer to the two outer rings, which are highly distorted from planarity. In contrast, the inner ring is essentially planar. As a consequence, the core size (C_t-N) of the inner ring is considerably smaller (2.02 Å) than those of the outer rings (2.08 Å). Nevertheless, the porphyrin rings in this complex are separated by distances comparable to those of the double deckers.[14d,e] This suggests that the magnitude of $\pi\pi$ interactions should be similar in the double- and triple-decker sandwiches. Thus, the triple-decker complexes afford the opportunity for investigating the effects of extending the π network to the next level of complexity from the prototypical dimeric systems.

In this paper, we report the results of a detailed spectroscopic and electrochemical investigation of three neutral and singly oxidized lanthanide triple-decker sandwich complexes $Ln_2(OEP)_3$ (Ln = La(III), Ce(III), Eu(III); OEP = octaethylporphyrin). The spectroscopic techniques include UV-vis, near-infrared (near-IR), infrared (IR), resonance Raman (RR), and electron paramagnetic resonance (EPR). On the basis of these studies, we propose a molecular orbital scheme that accounts for a number of the properties of the triple-decker complexes.

Table I. Half-Wave Potentials ($E_{1/2}$)[a] for the $Ln_2(OEP)_3$ Complexes

	redox couple ($E_{1/2}$)				
complex	$E_{1/2}^{4+/3+}$	$E_{1/2}^{3+/2+}$	$E_{1/2}^{2+/+}$	$E_{1/2}^{+/0}$	$E_{1/2}^{0/-}$
$La_2(OEP)_3$	+1.50	+1.15	+0.70	+0.30	-1.62
$Ce_2(OEP)_3$	+1.41	+1.11	+0.69	+0.24	-1.62
$Eu_2(OEP)_3$	+1.60	+1.21	+0.64	+0.18	-1.63

[a] Potentials listed are volts vs Ag/AgCl (saturated KCl).

(1) Hoffman, B. M.; Ibers, J. A. *Acc. Chem. Res.* **1983**, *16*, 15-21 and references therein.
(2) (a) Martinsen, J.; Stanton, J. L.; Greene, R. L.; Tanaka, J.; Hoffman, B. M.; Ibers, J. A. *J. Am. Chem. Soc.* **1985**, *107*, 6915-6920. (b) Ogawa, M. Y.; Martinsen, J.; Palmer, S. M.; Stanton, J. L.; Tanaka, J.; Greene, R. L.; Hoffman, B. M.; Ibers, J. A. *Ibid.* **1987**, *109*, 1115-1121.
(3) Turek, P.; Petit, P.; Andrē, J.-J.; Simon, J.; Even, R.; Boudjema, B.; Guillaud, G.; Maitrot, M. *J. Am. Chem. Soc.* **1987**, *109*, 5119-5122.
(4) Nohr, R. S.; Kuznesof, P. M.; Wynne, K. J.; Kenney, M. E.; Siebenman, P. G. *J. Am. Chem. Soc.* **1981**, *103*, 4371-4377.
(5) Diel, B. N.; Inabe, T.; Lyding, J. W.; Schoch, K. F., Jr.; Kannewurf, C. R.; Marks, T. J. *J. Am. Chem. Soc.* **1983**, *105*, 1551-1567.
(6) Pietro, W. J.; Marks, T. J.; Ratner, M. A. *J. Am. Chem. Soc.* **1985**, *107*, 5387-5391.
(7) Diel, B. N.; Inabe, T.; Taggi, N. K.; Lyding, J. W.; Schneider, O.; Hanack, M.; Kannewurf, C. R.; Marks, T. J.; Schwartz, L. H. *J. Am. Chem. Soc.* **1984**, *106*, 3207-3214.
(8) Collman, J. P.; McDevitt, J. T.; Leidner, C. R.; Yee, G. T.; Torrance, J. B.; Little, W. A. *J. Am. Chem. Soc.* **1987**, *109*, 4606-4614.
(9) Hale, P. D.; Pietro, W. J.; Ratner, M. A.; Ellis, D. E.; Marks, T. J. *J. Am. Chem. Soc.* **1987**, *109*, 5943-5947.
(10) Gouterman, M.; Holten, D.; Lieberman, E. *Chem. Phys.* **1977**, *25*, 139-153.
(11) (a) Hunter, C. A.; Sanders, J. K. M.; Stone, A. J. *Chem. Phys.* **1989**, *133*, 395-404. (b) Hunter, C. A.; Sanders, J. K. M. *J. Am. Chem. Soc.* **1990**, *112*, 5525-5534.
(12) Schick, G. A.; Schreiman, I. C.; Wagner, R. W.; Lindsey, J. S.; Bocian, D. F. *J. Am. Chem. Soc.* **1989**, *111*, 1344-1350.
(13) Osuka, A.; Maruyama, K. *J. Am. Chem. Soc.* **1988**, *110*, 4454-4456.
(14) (a) Buchler, J. W.; Kapellmann, H.-G.; Knoff, M.; Lay, K.-L.; Pfeifer, S. *Z. Naturforsch. B: Anorg. Chem., Org. Chem.* **1983**, *38B*, 1339-1345. (b) Buchler, J. W.; Knoff, M. In *Optical Properties and Structures of Tetrapyrroles*; Blauer, G., Sund, H., Eds.; de Gruyter: West Berlin, 1985; pp 91-105. (c) Buchler, J. W.; Elsässer, K.; Kihn-Botulinski, M.; Scharbert, B. *Angew. Chem., Int. Ed. Engl.* **1986**, *25*, 286-287. (d) Buchler, J. W.; De Cian, A.; Fischer, J.; Kihn-Botulinski, M.; Paulus, H.; Weiss, R. *J. Am. Chem. Soc.* **1986**, *108*, 3652-3659. (e) Buchler, J. W.; De Cian, A.; Fischer, J.; Kihn-Botulinski, M.; Weiss, R. *Inorg. Chem.* **1988**, *27*, 339-345. (f) Buchler, J. W.; Scharbert, B. *J. Am. Chem. Soc.* **1988**, *110*, 4272-4276. (g) Buchler, J. W.; Loffler, J. *Z. Naturforsch.* in press. (h) Buchler, J. W.; De Cian, A.; Fischer, J.; Hammerschmitt, P.; Loffler, J.; Scharbert, B.; Weiss, R. *Chem. Ber.* **1989**, *122*, 2219-2228. (i) Buchler, J. W.; Kihn-Botulinski, M.; Loffler, J.; Wicholas, M. *Inorg. Chem.* **1989**, *28*, 3770-3772.
(15) (a) Yan, X.; Holten, D. *J. Phys. Chem.* **1988**, *92*, 409-414. (b) Bilsel, O.; Rodriguez, J.; Holten, D. *J. Phys. Chem. 94*, 3508-3512. (c) Bilsel, O.; Rodriguez, J.; Holten, D.; Girolami, G. S.; Milam, S. N.; Suslick, K. S. *J. Am. Chem. Soc.* **1990**, *112*, 4075-4077.
(16) (a) Girolami, G.; Milam, S.; Suslick, K. *Inorg. Chem.* **1987**, *26*, 343-344. (b) Girolami, G.; Milam, S.; Suslick, K. *J. Am. Chem. Soc.* **1988**, *110*, 2011-2012.
(17) (a) Donohoe, R. J.; Duchowski, J. K.; Bocian, D. F. *J. Am. Chem. Soc.* **1988**, *110*, 6119-6124. (b) Duchowski, J. K.; Bocian, D. F. *J. Am. Chem. Soc.* **1990**, *112*, 3212-3318. (c) Perng, J.-H.; Duchowski, J. K.; Bocian, D. F. *J. Phys. Chem.* **1990**, *94*, 6684. (d) Duchowski, J. K.; Bocian, D. F. *Inorg. Chem.* in press.

0002-7863/90/1512-8807$02.50/0

Table II. UV-Vis Spectral Data for $Ln_2(OEP)_3$ and $Ln_2(OEP)_3^+$ Complexes[a]

$La_2(OEP)_3$	386[b] (5.29)[c]	530 (4.27)	567 (4.03)	629 (3.83)	728 (3.59)
$La_2(OEP)_3^+$	373 (5.13)	530 (3.96)	567 (3.86)	~2200 (~3.17)[d]	
$Ce_2(OEP)_3$	387 (5.28)	529 (4.24)	568 (4.14)	631 (3.85)	743 (3.59)
$Ce_2(OEP)_3^+$	367 (5.13)	521 (3.97)	561 (4.10)	~2200 (~3.17)[d]	
$Eu_2(OEP)_3$	382 (5.25)	530 (4.03)	572 (3.92)	658 (3.67)	800 (3.05)
$Eu_2(OEP)_3^+$	363 (5.09)	527 (3.79)	562 (3.98)	~2200 (~3.17)[d]	

[a] In CH_2Cl_2 solutions. [b] λ_{max} in nanometers. [c] log ϵ. [d] In KBr pellets.

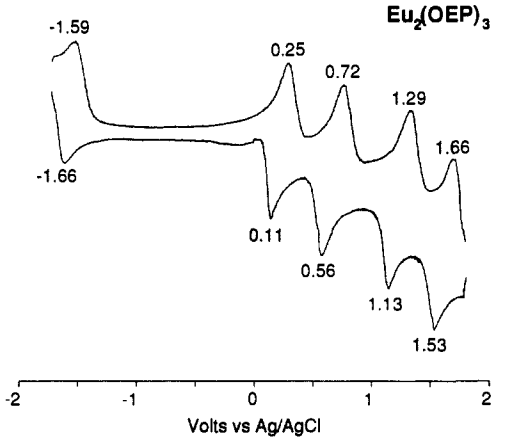

Figure 1. CV of $Eu_2(OEP)_3$ in CH_2Cl_2, 0.1 M TBAH.

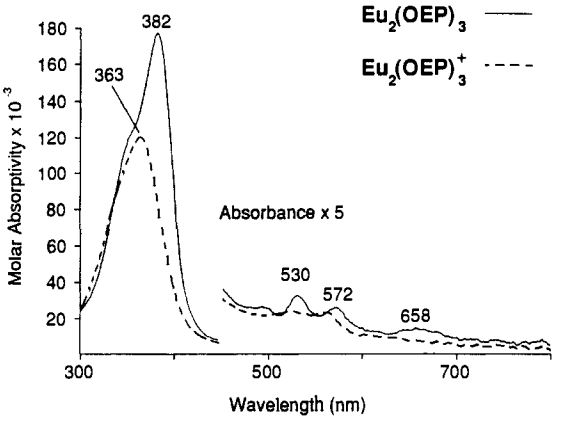

Figure 2. UV-vis absorption spectra of the neutral (—) and singly oxidized (---) $Eu_2(OEP)_3$ complex in CH_2Cl_2.

II. Experimental Section

The neutral $Ln_2(OEP)_3$ complexes were prepared according to the procedure of Buchler and co-workers.[14b,d,e,i] The identity of the complexes was confirmed via UV-vis and nuclear magnetic resonance spectroscopy. Chemical oxidations were carried out with phenoxathiinylium hexachloroantimonate in 1,2-dichloroethane (Aldrich, 99+%) under an inert atmosphere.[18] Electrochemical oxidations were performed in CH_2Cl_2 solutions in a Vacuum Atmospheres Model HE-43 drybox with use of procedures and instrumentation previously described.[19] Tetrabutylammonium hexafluorophosphate, TBAH (Aldrich, recrystallized twice from absolute ethanol), was used as the supporting electrolyte. The oxidized samples were typically ~1 mM complex and 0.1 M TBAH. Purification of the neutral and oxidized complexes was performed according to the procedures of Buchler et al.[14c,d,e,i]

Absorption spectra were collected on a Perkin-Elmer 330 grating spectrophotometer. The samples were dissolved in CH_2Cl_2 or suspended in a supporting medium of KBr (1:200 ratio). Infrared spectra of the samples in KBr pellets were recorded on a Nicolet FT 5DXB spectrometer. The spectral slit width was 2 cm^{-1}.

RR spectra were acquired with use of instrumentation described elsewhere.[19] The samples were dissolved in dry, degassed CH_2Cl_2 or suspended in compressed pellets with a supporting medium of Na_2SO_4. The incident laser powers were approximately 35 or 50 mW for B- or Q-region excitation, respectively. The spectral slit width was 3 cm^{-1}.

EPR spectra were acquired on a Bruker ER-300 X-band spectrometer equipped with liquid N_2 and He accessories. Neutral and chemically oxidized complexes were dissolved in dry, degassed CH_2Cl_2 solutions. Electrochemically oxidized samples were aliquoted directly from the electrochemical cell into quartz EPR cells equipped with ground-glass joints. Room-temperature spectra were acquired in a flat cell. The microwave power was typically 1 mW.

III. Results

A. Electrochemistry. The cyclic voltammogram (CV) of a representative triple decker, $Eu_2(OEP)_3$, is shown in Figure 1. The four waves on the positive side correspond to successive ring-centered oxidations, while the single wave on the negative side corresponds to a ring-centered reduction.[17a,20] The CVs of $La_2(OEP)_3$ and $Ce_2(OEP)_3$ are similar to those shown in Figure 1. However, in the case of the latter complex, two additional oxidation waves are observed at 0.80 and 0.95 V. These probably correspond to metal-centered oxidations. The potentials for the ring-centered oxidations and reductions of all three $Ln_2(OEP)_3$ complexes are summarized in Table I. Inspection of the table reveals that the first oxidations for the three complexes occur in the range 0.18–0.30 V. These potentials are considerably cathodic of those exhibited by monomeric LnOEP complexes (~0.7 V) and reflect the effects of strong $\pi\pi$ interactions.[17a] This type of redox destabilization is also characteristic of $Ln(OEP)_2$ systems.[14f] For these double deckers, the first oxidations become more cathodic as the size of the central metal ion decreases. This is also the case for the triple deckers investigated here.

B. Absorption Spectra. The absorption spectra of $Eu_2(OEP)_3$ and $Eu_2(OEP)_3^+$ are compared in Figure 2. The absorption data for these and the other two neutral and oxidized $Ln_2(OEP)_3$ complexes are given in Table II. The Soret maxima of all the singly oxidized species are blue-shifted relative to those of their neutral counterparts. These spectral shifts are characteristic of porphyrin π-cation-radical formation.[20] A particularly noteworthy aspect of the absorption spectra of the cations is that they do not appear to be comprised of features associated with separate neutral and oxidized chromophores isolated within a single molecule. This indicates that the redox orbital is delocalized over all three rings in the triple-decker system. Delocalization due to strong $\pi\pi$ interactions has also been observed for all the symmetrical double-decker lanthanide porphyrin sandwiches investigated thus far.[17a-c] The delocalization is not influenced by the metal ion in single-hole $Ln(OEP)_2$ complexes because the hole resides in an a_{1u}-derived porphyrinic molecular orbital that is both spacially removed from the orbitals of the metal ion and symmetrically inappropriate to mix with these orbitals.[17a,b]

A prominent feature of all single-hole double-decker lanthanide porphyrin sandwich complexes is a near-IR absorption band that lies in the range 1100–1400 nm depending on the metal ion and/or the peripheral substituents on the porphyrin ring.[14f,17b,c] Examination of this spectral region of the $Ln_2(OEP)_3^+$ complexes failed to reveal a corresponding absorption band. However, a broad, featureless, moderately strong absorption is observed in the very low-energy region of the near-IR spectrum of these complexes ~2200 nm (4600 cm^{-1}). This absorption feature is shown in Figure 3, which compares the spectra of $Eu_2(OEP)_3$ and $Eu_2(OEP)_3^+$. As can be seen, the maximum intensity of this cation band is approximately 3 times greater than that of the CH stretching modes of the ethyl substituents (ca. 2900 cm^{-1}). In the case of the single-hole, double-decker lanthanide porphyrin sandwiches, the position of the near-IR band is sensitive to the

(18) Gans, P.; Marchon, J.-C.; Reed, C. A.; Regnard, J.-R. *Nouv. J. Chim.* **1981**, *5*, 203–204.
(19) Donohoe, R. J.; Atamian, M.; Bocian, D. F. *J. Am. Chem. Soc.* **1987**, *109*, 5593–5599.
(20) Felton, R. H. In *The Porphyrins*; Dolphin, D., Ed.; Academic Press: New York, 1978; Vol. V, pp 53–125.

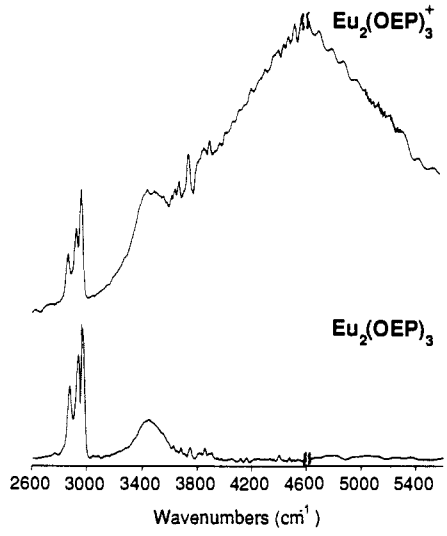

Figure 3. Near-IR absorption spectra of the neutral (bottom) and singly oxidized (top) $Eu_2(OEP)_3$ complex in KBr pellets. The sharp bands near 2900 cm^{-1} are due to the CH stretches of the ethyl substituents. The broad band near 3500 cm^{-1} is due to residual H_2O. The sharp features on the broad band of the cation are attributed to instrument noise. The spectra on the high- and low-energy sides of 4600 cm^{-1} (note break) were recorded on two different spectrometers.

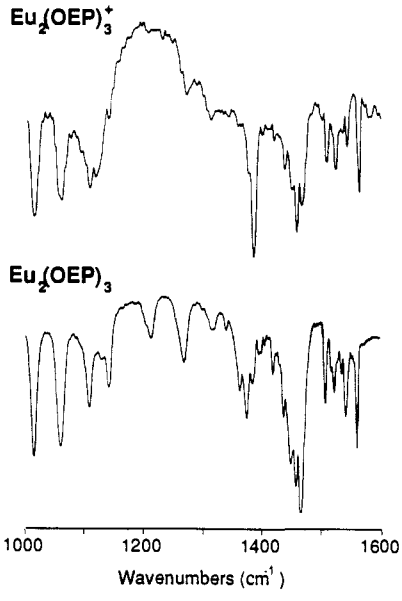

Figure 4. IR spectra of the neutral (bottom) and singly oxidized (top) $Eu_2(OEP)_3$ complex in KBr pellets.

size of the central metal ion.[14f] Because of the breadth and shape of this band, we were not able to ascertain whether such a trend occurs for the triple-decker cations. Consequently, the same value of λ_{max} (log ϵ) is listed for all three complexes in Table II.

C. IR Spectra. The mid-IR spectra of $Eu_2(OEP)_3$ and $Eu_2(OEP_3^+)$ are compared in Figure 4. The spectra of the neutral and oxidized La(III) and Ce(III) complexes are similar to those shown in the figure. Although the IR spectra of the neutral and oxidized complexes are not identical, there are no obvious features in the spectra of the cations that can be associated with characteristic oxidation marker bands (typically near 1300 and 1500 cm^{-1}).[21]

D. RR Spectra. The high-frequency regions of the B- and Q-state excitation RR spectra of $Eu_2(OEP)_3$ are shown in the bottom traces of Figures 5 and 6, respectively. Examination of the 1500–1625-cm^{-1} spectral region of the neutral complex reveals that the ν_2 (ca. 1585 cm^{-1}), ν_{10} (ca. 1610 cm^{-1}), and ν_{11} (ca. 1550

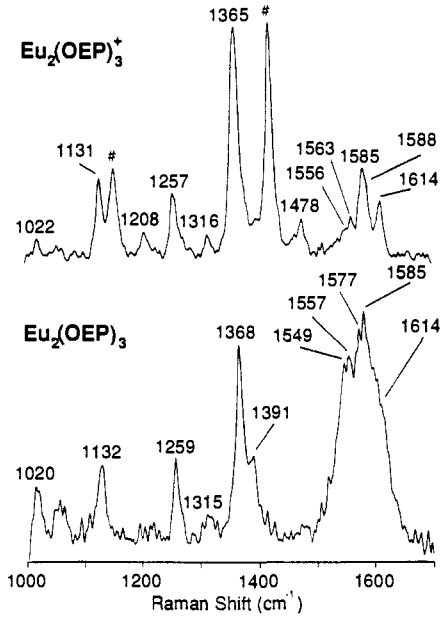

Figure 5. High-frequency regions of the B-state excitation (λ_{ex} = 406.7 nm) RR spectra of the neutral (bottom) and singly oxidized (top) $Eu_2(OEP)_3$ complex in CH_2Cl_2 solutions. The solvent bands are indicated by the symbol #.

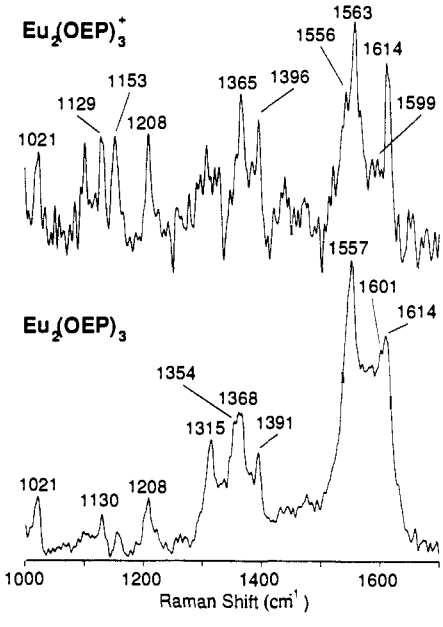

Figure 6. High-frequency regions of the Q-state excitation (λ_{ex} = 530.9 nm) RR spectra of the neutral (bottom) and singly oxidized (top) $Eu_2(OEP)_3$ complex in Na_2SO_4 pellets.

cm^{-1}) bands appear to be doubled. Polarization measurements indicate that each member of a given doublet has a similar depolarization ratio. This doubling is observed for all three neutral triple deckers in both solution- and solid-state spectra. The frequencies of the bands assigned as doublets are also reproducible in separate spectra acquisitions, which indicates that these particular bands are not due to spectral noise. Such doubling is not observed for lanthanide porphyrin monomers or double deckers.[17a-c] The most likely explanation for this effect is that the two sets of bands are due to the structural inequivalence of the inner and outer rings of the triple-decker sandwich.[14d] Because C_t–N is larger for the outer rings than for the inner ring, the core size sensitive RR bands of the former macrocycles are expected to occur at lower frequencies.[22] We have assigned the two sets of RR bands

(21) Shimoura, E. T.; Phillipi, M. A.; Goff, H. M.; Scholtz, W. F.; Reed, C. A. *J. Am. Chem. Soc.* **1981**, *103*, 6778–6780.

(22) Oertling, W. A.; Salehi, A.; Chung, Y. C.; Leroi, G. E.; Chang, C. K.; Babcock, G. T. *J. Phys. Chem.* **1987**, *91*, 5887–5898.

Table III. Resonance Raman Frequencies (cm^{-1}) of the $Ln_2(OEP)_3$ and $Ln_3(OEP)_3^+$ Complexes

	$La_2(OEP)_3$		$La_2(OEP)_3^+$		$Ce_2(OEP)_3$		$Ce_2(OEP)_3^+$		$Eu_2(OEP)_3$		$Eu_2(OEP)_3^+$	
	inner	outer	inner	outer	inner	outer	inner	outer	inner	outer	inner	outer
ν_{10}		1600		1600	1610	1601		1600	1614	1601	1614	1599
ν_2	1578	1572	1586	1581	1580	1576	1584	1580	1585	1577	1588	1585
ν_{11}	1557	1547	1561	1554	1554	1547	1558	1565	1557	1549	1563	1556

	difference in frequency between $Ln_2(OEP)_3$ and $Ln_2(OEP)_3^+$					
	inner	outer	inner	outer	inner	outer
$\Delta\nu_{10}$		0		−1	0	−2
$\Delta\nu_2$	+8	+9	+4	+4	+3	+8
$\Delta\nu_{11}$	+4	+7	+4	+8	+6	+7

accordingly. These spectral assignments are summarized for all three neutral triple deckers in Table III.

The high-frequency regions of the B- and Q-state excitation RR spectra of $Eu_2(OEP)_3^+$ are shown in the top traces of Figures 5 and 6, respectively. As is the case for the neutral complex, the ν_2 and ν_{11} bands of the cation are doubled. The former modes are at 1585 and 1588 cm^{-1}, while the latter are at 1556 and 1563 cm^{-1}. The assignment of the inner- and outer-ring modes is not obvious. If the 1585- and 1556-cm^{-1} bands are associated with the inner ring, this would indicate that the ν_2 and ν_{11} modes of this ring do not shift upon oxidation while those of the outer rings upshift by 11 and 14 cm^{-1}, respectively (Table III). On the other hand, if this pair of bands is associated with the outer rings, this would indicate that the RR bands of both the inner and outer rings shift. In this case, the ν_2 and ν_{11} modes of the inner ring would upshift by 3 and 6 cm^{-1}, respectively, while those of the outer rings would upshift by 8 and 7 cm^{-1}, respectively. The first interpretation of the RR data would suggest that the hole is delocalized over both outer rings while the inner ring remains neutral. The second interpretation would suggest that the hole is delocalized over all three rings. Inasmuch as the latter explanation is most consistent with the optical spectroscopic data, we have assigned the inner- and outer-ring modes of all three triple-decker cations on this basis. These assignments are summarized in Table III. The oxidation-induced spectral shifts of the RR bands are also given in the table. The positive shifts observed for the ν_2 and ν_{11} bands of all three cations are consistent with an a_{1u}-based redox orbital, as expected for metallooctaethylporphrin complexes.[22,23]

E. EPR Spectra. No EPR signals were observed for the neutral $Ln_2(OEP)_3$ complexes at room or cryogenic temperatures. Signals are not expected for the La(III) complex because it is diamagnetic. On the other hand, both the Eu(III) and Ce(III) complexes are paramagnetic.[14d,e,i] The absence of signals from these complexes could be due to a number of factors such as coupling between the ions or fast relaxation. In the case of $Ce_2(OEP)_3^+$ and $La_2(OEP)_3^+$, EPR signals are observed at room temperature, while no signals are observed for $Eu_2(OEP)_3^+$. The spectra of the former two complexes (not shown) are narrow (width ≈ 6–10 G) first derivatives centered near $g = 2.00$ with no resolved hyperfine. Such signals are characteristic of a_{1u}-like porphyrin cation radicals.[24] Spectra recorded at cryogenic temperatures also failed to reveal any hyperfine structure; however, for $Ce_2(OEP)_3^+$, the signal becomes slightly anisotropic ($g = 2.00$ and 2.01). At temperatures below 200 K, EPR signals are observed for $Eu_2(OEP)_3^+$. The spectrum (not shown) is a broad (width ≈ 60 G) first derivative centered near $g = 2.07$ with no resolved hyperfine. The breadth of the signal most likely reflects the presence of g-value anisotropy and/or hyperfine interactions between the unpaired electron and the metal ion.[14e]

IV. Discussion

The spectroscopic data presented herein are most consistent with a model in which there are very strong $\pi\pi$ interactions between the porphyrin macrocycles of the $Ln_2(OEP)_3$ complexes.

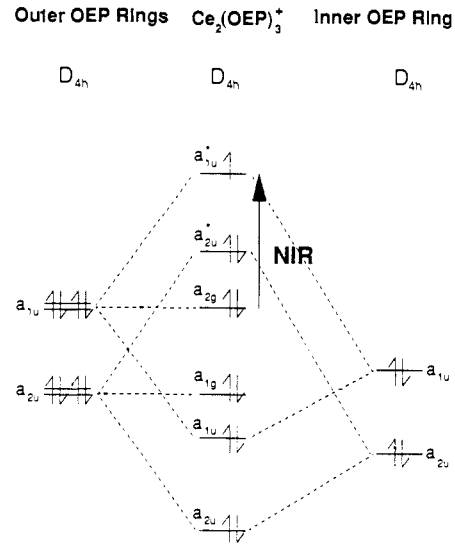

Figure 7. Partial MO diagram from the triple-decker sandwich complexes. The intratrimer transition that gives rise to the near-IR absorption involves promotion of an electron from an a_{2g} (nonbonding) to an a_{1u}^* (antibonding) orbital and is labeled accordingly (see text).

Such interactions provide a mechanism for the destabilization of the redox orbital of these systems relative to that of lanthanide porphyrin monomers. The systematic increase in the extent of destabilization ($E_{1/2}$, Eu < Ce < La) with the decrease in the radius of the lanthanide ion is further consistent with this picture because the separation between the porphyrin π systems decreases as the metal ion radius is reduced.[14f] The presence of strong $\pi\pi$ interactions also leads to the appearance of the low-energy absorption band (ca. 2200 nm) in the $Ln_2(OEP)_3^+$ complexes (vide infra). In fact, the magnitude of the interactions is sufficiently large that the holes in all the triple-decker cations are delocalized over the three rings on the vibrational and electronic time scales. Hole delocalization accounts for the appearance of a single set of bands in the UV–vis spectra of these cations. It also accounts for the magnitude of the oxidation-induced shifts of the RR bands of these complexes relative to those of either double-decker or monomeric lanthanide porphyrins.[17a,b] In this regard, the RR-band shifts observed for the inner and outer rings of the triple deckers are comparable to one another and smaller than those of either the double deckers or the monomers. By presuming that the frequencies of the RR bands of the inner and outer rings are approximately equally shifted by the removal of a given amount of charge, this suggests that oxidation removes the equivalent of $\sim^1/_3$ electron from each ring of the triple decker. In the case of the double-decker sandwiches, the equivalent of $^1/_2$ electron is removed from each ring upon oxidation. The fact that a relatively small amount of hole density resides on each ring of the $Ln_2(OEP)_3^+$ complexes could also explain the absence of a strong cation-marker band in the mid-IR spectra.

In the limit of strong $\pi\pi$ interactions, a molecular orbital (MO) framework provides the most appropriate description of the electronic structure of the π assembly.[17a] A partial MO diagram for the triple-decker systems is shown in Figure 7. For clarity, only those MOs derived from the a_{1u} and a_{2u} orbitals of the

(23) Czernuszewicz, R. S.; Macor, K. A.; Li, X.-Y.; Kincaid, J. R.; Spiro, T. G. *J. Am. Chem. Soc.* **1989**, *111*, 3860–3869.

(24) Fajer, J.; Davis, M. S. In *The Porphyrins*; Dolphin, D., Ed.; Academic Press: New York, 1978; Vol. IV, pp 197–256.

individual rings are shown. The left and right sides of the figure show the orbitals of the outer and inner OEP rings, respectively, in the limit of zero porphyrin–porphyrin interaction. The middle of the diagram shows the MOs of the triple decker in the limit of strong $\pi\pi$ interaction. The orbitals of the constituent monomers are energetically ordered in a fashion appropriate for OEP and labeled according to D_{4h} symmetry.[24] The outer- and inner-ring orbitals are energetically ordered (outer rings higher) in a manner consistent with the structural and spectroscopic data (vide infra). The MOs of the triple decker are also labeled according to D_{4h} symmetry, which is the approximate symmetry of the complex (an $\sim 45°$ rotation of the inner ring with respect to the eclipsed outer rings).[14d] The exact energies and splittings of the MOs derived from the a_{1u} and a_{2u} monomer orbitals are not known and have been ordered for pictorial clarity. Oxidation results in a hole in an a_{1u}-derived triple-decker MO (see sections III.D and III.E); consequently, the appropriate a_{1u}-derived MO is given the highest energy.

In the triple-decker sandwiches, strong interactions between the monomer orbitals of appropriate symmetry result in bonding, nonbonding, and antibonding MOs as shown in Figure 7. In the limit that the monomer orbitals are equivalent, the bonding and antibonding triple-decker MOs contain contributions from all three rings (50% from the inner ring and 25% from each of the outer rings, neglecting the explicit effects of overlap). The nonbonding MOs are derived only from orbitals of the outer rings. In the triple deckers, however, the inner and outer rings are structurally inequivalent such that the metal ions are closer to the latter macrocycles.[14d] This should tend to destabilize the orbitals of outer rings relative to those of the inner ring inasmuch as LnOEP complexes are easier to oxidize than H_2OEP.[17a,20] In addition, there is evidence that highly nonplanar porphyrins (outer rings) are more easily oxidized than planar macrocycles (inner rings).[25] As shown in Figure 7, both of these effects would tend to increase the outer-ring contribution to the redox orbital in the triple deckers. This view is in accord with the observed relative magnitudes of the oxidation-induced shifts of the inner- and outer-ring RR bands, which suggest a redox orbital composition of $\sim 33\%$ from each of the constituent porphyrin macrocycles. Obviously, other factors (besides metal ion proximity) that render the inner and outer rings inequivalent may also contribute to the exact composition of the redox orbital in the triple-decker sandwich complexes.

The MO scheme in Figure 7 provides an explanation for the very low energy absorption band (ca. 2200 nm (4600 cm^{-1})) observed for the $Ln_2(OEP)_3^+$ complexes. In this scheme, promotion of an electron from the filled nonbonding a_{2g} orbital to the half-filled antibonding a_{1u}^* orbital represents a z-polarized, allowed electronic transition. This transition moves electron density from the regions between the inner and outer rings (strong overlap) to the top and bottom of the sandwich (zero overlap). We have previously proposed that the near-IR absorption band (ca. 1250 nm (8000 cm^{-1})) observed in single-hole, double-decker sandwiches[14f] is due to transitions between filled and half-filled MOs.[17] These MOs are derived from the highest occupied orbitals of the constituent monomers and are split by the strong $\pi\pi$ interactions in the double deckers. In the latter complexes, however, the transition is between bonding and antibonding MOs. If the magnitude of $\pi\pi$ interactions is similar in the double and triple deckers, the splitting between the bonding and antibonding MOs of the former would necessarily be larger than that between the nonbonding and antibonding MOs of the latter. This is in accord with a higher energy near-IR absorption feature in the double-decker sandwiches.[14f] In this regard, the first oxidation potential of $Ce^{IV}(OEP)_2$ is comparable[17a] to that of the $Ln_2(OEP)_3$ complexes, which indicates a similar extent of redox orbital destabilization in the double and triple deckers (relative to a lanthanide porphyrin monomer). [The first oxidation potentials of the $Ln^{III}(OEP)_2$ complexes cannot serve as a comparison because these neutral sandwiches contain a hole in the porphyrin π system.[14f]] This would suggest that the splitting between the bonding and antibonding MOs of the $Ln(OEP)_2$ complexes should be approximately twice as large as that between the nonbonding and antibonding MOs of the $Ln_2(OEP)_3$ sandwiches. Accordingly, the near-transition of the double deckers should occur at approximately twice the energy of that of the triple deckers as is, in fact, observed. Collectively, these observations lend further support to the qualitative validity of the simple MO scheme we have proposed for both the double- and triple-decker lanthanide porphyrin sandwich complexes.

Acknowledgment. We thank Professor D. Holten for helpful discussions and Mr. K. Constantine for aid in obtaining the NMR spectra. This work was supported by a grant to D.F.B. from the National Institute of General Medical Sciences (GM-36243).

(25) Barkigia, K. M.; Chantranupong, L.; Smith, K. M.; Fajer, J. *J. Am. Chem. Soc.* **1988**, *110*, 7566–7567.